SCIENTIFIC REPORTS

OPEN

SUBJECT AREAS:
GEOCHEMISTRY
MID-INFRARED PHOTONICS

Received
20 December 2013

Accepted
26 August 2014

Published
31 October 2014

Correspondence and requests for materials should be addressed to B.P. (Bobby.Pejcic@csiro.au) or B.M. (Boris.Mizaikoff@uni-ulm.de)

Infrared Attenuated Total Reflectance Spectroscopy: An Innovative Strategy for Analyzing Mineral Components in Energy Relevant Systems

Christian Menno Müller[1,2], Bobby Pejcic[1], Lionel Esteban[1], Claudio Delle Piane[1], Mark Raven[3] & Boris Mizaikoff[2]

[1]CSIRO, Energy Flagship, 26 Dick Perry Ave, Kensington, WA, Australia, 6151, [2]University of Ulm, Institute of Analytical and Bioanalytical Chemistry, Albert-Einstein-Allee 11, 89081 Ulm, Germany, [3]CSIRO, Land and Water, Waite Campus, Glen Osmond, SA, 5064 Australia.

The direct qualitative and quantitative determination of mineral components in shale rocks is a problem that has not been satisfactorily resolved to date. Infrared spectroscopy (IR) is a non-destructive method frequently used in mineral identification, yet challenging due to the similarity of spectral features resulting from quartz, clay, and feldspar minerals. This study reports on a significant improvement of this methodology by combining infrared attenuated total reflection spectroscopy (IR-ATR) with partial least squares (PLS) regression techniques for classifying and quantifying various mineral components present in a number of different shale rocks. The developed multivariate classification model was calibrated using pure component mixtures of the most common shale minerals (i.e., kaolinite, illite, montmorillonite, calcite, and quartz). Using this model, the IR spectra of 11 real-world shale samples were analyzed and evaluated. Finally, the performance of the developed IR-ATR method was compared with results obtained via X-ray diffraction (XRD) analysis.

In recent years, there has been an increased interest in exploring and commercially exploiting gas reserves hosted by shale rocks to meet future global energy needs[1,2]. Shales are a group of sedimentary rock that consist of fine grain mineral particles mixed with organic matter, which has significant potential as a natural source of hydrocarbon. The organic matter fractions in shales may have various origins, and the abundance, type, and thermal maturity may also vary significantly[3]. In particular, oil shales contain large quantities of organic material as kerogen, which is a complex mixture of insoluble hydrocarbons derived from decomposed plant and animal matter. In contrast, gas shales consist of natural gas, which is adsorbed/absorbed at or into the organic matter fraction or trapped in between the mineral particles. The mineral constituents and the general rock properties play a crucial role whether a particular shale is economically viable, and whether useful quantities of gas and/or oil may be harvested from this composite[4]. Although the mineral content may vary widely, most shales are typically composed of variable amounts of clays along with quartz, carbonates, feldspars, and iron oxides as the most prominent constituents[5]. Understanding the relationship between shale composition and the geological factors that govern gas/oil production is an issue that has not been satisfactorily addressed.

A detailed physical and chemical characterization of shale rocks is therefore a crucial aspect for understanding and minimizing exploration risks, and for optimizing harvesting and production strategies. Josh and co-workers recently described a series of laboratory methods (i.e., mercury, injection porosimetry, X-ray computer tomography, and ultrasonic methods) commonly applied for determining the physical and mechanical properties (i.e., porosity, permeability, dielectric, elasticity, and mechanical strength) of shales[6]. On the other hand, mineral identification and quantifying the mineral content requires specific analytical techniques providing additional chemical information. X-ray diffraction (XRD) is the most commonly applied tool providing extensive information on the chemical and mineral composition of shale rocks[7–9]. As the X-ray diffraction pattern is unique for each crystalline constituent, identification may be achieved by determining the interplanar spacing/distance of the crystal via the Bragg equation, and comparing the obtained result with comprehensive powder diffraction databases (e.g., International Centre for Diffraction Data). In fact, XRD is a well-established standard method

for mineral identification and characterization, and a number of papers have been published showing that it provides invaluable quantitative information of complex multi-component mixtures such as shales[10,11]. However, the presence of certain clays along with various natural organic matter and amorphous components may give rise to quantitative errors, which need to be considered and/or corrected[8–10]. In some cases the shale samples are treated with different solutions/chemicals to remove various components and to improve the identification of certain clay minerals[11]. Consequently, a complete chemical characterization of shale rocks is apparently not feasible using only XRD, and complementary methods such as thermogravimetry (TGA) or infrared spectroscopy (IR) are required[12–14].

Fourier transform infrared (FTIR) spectroscopy is an optical technique that has been used for characterizing a wide range of minerals[13,15–17]. Compared to XRD, IR spectroscopy is rapid, and capable of providing both chemical and structural information on a wide range of amorphous, semicrystalline, and crystalline materials. In particular, IR spectroscopy is attractive for analyzing shales, as information on the organic matter fraction is directly accessible[18,19], and simultaneously providing discriminatory information on the different types of minerals present within the sample[18,20,21].

A variety of measurement techniques are available for collecting spectra in the mid-infrared (MIR; 3–20 μm) spectral region. Among the conventional methods used for sample preparation during shale characterization has been the preparation of pressed KBr pellets[19,21,22]. In this procedure, a small quantity of sample (typically a few mg) is dispersed within an IR-transparent KBr matrix by hand in a mortar, and then compacted into a pellet for IR transmission-absorption analysis. Although KBr pellets are highly useful for analyzing small sample quantities, several issues such as particle agglomeration, water absorption, reproducible mixing[22], particle size effects[21] and weighing errors[13] limit reliable quantitative analysis. Most of these problems can be avoided and/or minimized by using appropriate procedures (i.e., reducing the particle size to < 2 μm, minimizing water absorption by KBr by heating at $>110^{\circ}$C, ensuring proper homogenization of sample and KBr, etc.), and it has been shown that if these practices are adopted then reliable quantitative data can be obtained[23]. However, Kaufhold et al.[13] studied many different clays and concluded that the IR method based on KBr pellets is not a suitable substitute for XRD characterization and quantification.

To avoid some of these sample preparation artefacts, reflectance methods including diffuse reflectance infrared Fourier transform (DRIFT) spectroscopy[7], and infrared attenuated total reflectance (IR-ATR) spectroscopy have been evaluated for characterizing oil shales[24]. In particular, Palayangoda and Nguyen recently showed that IR-ATR in combination with principal component regression may be used to provide quantitative information on some mineral constituents of oil shales[24]. Although only synthetic oil shale samples were prepared and used in this study, the chemometrics approach appeared promising. Other studies have revealed that IR-ATR spectroscopy may readily discriminate between bentonites of different origin[25].

However, despite a number of reports on the utility of IR spectroscopy for the characterization of shale rocks, comparatively few results have been published using ATR methods for quantifying the mineral composition of natural samples collected from shale formations. Hence, the objective of the present study was to evaluate the performance of IR-ATR spectroscopy for the qualitative and quantitative analysis of relevant mineral constituents present in natural shale rocks, and comparing the obtained data with XRD analysis results. Although IR is able to provide information concerning the oil yield[26], the organic matter/total organic carbon content[27], and the kerogen type[28] the focus of the present paper was to investigate the fundamental suitability of IR-ATR in conjunction with partial least squares (PLS) regression for quantifying the mineral components in natural shale samples. Currently, no suitable IR based method exists for accurately determining the mineralogical composition of shales. We believe that if IR spectroscopy is to be embraced by the scientific community in providing accurate quantitative information of shale rocks then further research is needed to develop appropriate methods for distinguishing the many different mineral constituents that occur in such complex natural materials. The overall aim is to develop a portable ATR based infrared technology that can be deployed in the field to provide rapid and reliable information concerning the chemistry of energy-related resources in geological systems.

Results

Qualitative analysis. In the first phase of this study, infrared spectra were collected on a small number of minerals that usually occur in shale rocks. According to several reports[18,22,29], quartz, clays (i.e., kaolinite, illite, and montmorillonite), carbonates (i.e., calcite and dolomite,) and feldspars (i.e., albite and orthoclase) are common minerals occurring in shales, and were selected as reference minerals for qualitative and quantitative analysis of natural shale samples. **Figure 1a**) illustrates a typical spectrum of quartz. The major absorption features of quartz are the peaks in the range of 1200 to 900 cm^{-1} assigned to the asymmetric stretching vibration of the Si–O groups with a peak maximum at 1080 cm^{-1}, the symmetric stretch at 800 and 780 cm^{-1}, and the symmetric and asymmetric Si–O bending mode at 695 cm^{-1}, 520 cm^{-1}, and 450^{-1}, respectively[30].

The spectra of clay minerals are shown in **Figure 1b**). To highlight the important features within clay mineral spectra, spectral regions without relevant signatures, e.g., 3500 to 1800 cm^{-1} were omitted here. IR spectra of clay minerals are usually characterized by three main areas: (i) the stretching and bending vibrations of the inner surface –OH groups observed in the region of 3700 to 3600 cm^{-1}, (ii) the stretching and bending vibrations of the Si–O groups, and (iii) the Si–O–M (with M = Al, Mg, etc.) vibrations with (ii) and (iii) extending from 1200 to 400 cm^{-1} [31].

The illite sample used in the present study contains 28% quartz, and therefore, several signals are overlapping or may be assigned to typical vibrations of quartz. Additional peaks are located at 3630 cm^{-1} and 828 cm^{-1}, and were assigned to the stretching vibrations of the –OH groups in the octahedral sheet, and the Al–OH–Mg vibration, respectively[32,33]. Furthermore, a shoulder arising from the Al–OH–Al bending vibration is evident at 915 cm^{-1} [31].

As water-bearing mineral, the most distinct features evident within the montmorillonite spectra are the bending vibration of the OH group at 1635 cm^{-1} [16]. Otherwise, the spectra of montmorillonite are similar to illite with only subtle differences of the spectral features. A weak shoulder at 885 cm^{-1} is attributed to the Fe–Al–OH vibration, which is not as recognizable in the illite spectrum. Further peaks such as e.g., the Al–OH–Al stretching vibration at 3625 cm^{-1}, and the broad Si–O asymmetric stretch feature from 1200 to 900 cm^{-1} have already been described[31].

The IR spectrum of kaolinite is very well described in literature[34]. Kaolinite is readily discriminated against other clay minerals herein due to its unique pattern in the spectral region of the inner surface –OH vibrations. Four clearly distinctive peaks at 3695 cm^{-1}, 3670 cm^{-1}, 3650 cm^{-1}, and 3620 cm^{-1} are attributed to the in-phase and out-of-phase motion modes, and to the stretching vibration of inner-surface –OH groups[35].

The spectra of the feldspar minerals albite and orthoclase are shown in **Figure 1c**). The albite spectrum displays multiple broader, yet partly overlapping absorption features ranging from 1200 to 900 cm^{-1}, 800 to 700 cm^{-1}, and 650 to 375 cm^{-1}. A detailed assignment of the fundamental vibrations is given elsewhere[36].

The orthoclase sample used in the present study contained 16 wt% of albite. This, and the fact that albite and orthoclase have only minor compositional differences leads to an almost identical IR spectrum

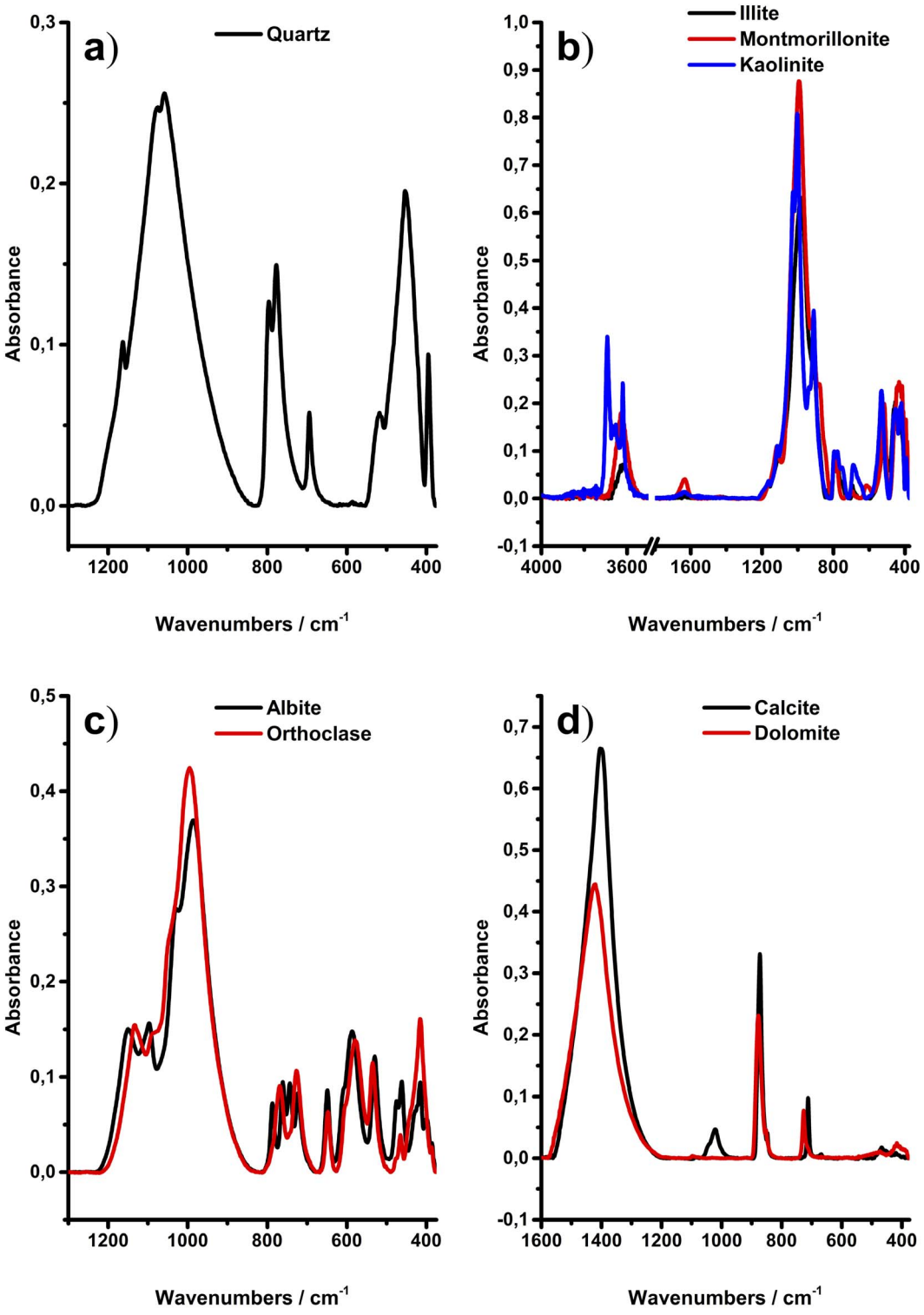

Figure 1 | **Infrared spectra of the mineral standards used in the IR-ATR study.**

with little features to discriminate these feldspars. However, successful attempts have already been reported for discriminating feldspar minerals using IR spectroscopy[37].

Figure 1d) shows the carbonate minerals calcite and dolomite. The fundamental vibrations arise from the carbonate CO_3^{2-} ion, and are assigned to the asymmetric stretch (ν_3) at 1400 cm^{-1} and the out-of-plane bending (ν_2) vibration at 875 cm^{-1}; these are considered the most prominent absorption features within carbonate spectra[38]. The peaks resulting from the in-plane bending vibration (ν_4) at 712 cm^{-1} and 727 cm^{-1} may be used to discriminate calcite from dolomite, respectively[39]. The absorption feature located at 1020 cm^{-1} is resulting from the in plane Si–O–Si stretch vibration caused by a talc impurity[40]. Hence, all mineral spectra obtained herein are well understood and are in agreement with literature.

The shales studied herein are natural samples, retrieved from deep wells, and hence, comprise substantial variety of mineral phases, and occasionally even remains of organic matter. Therefore, prior to IR spectral analysis, all shales were extensively characterized via XRD.

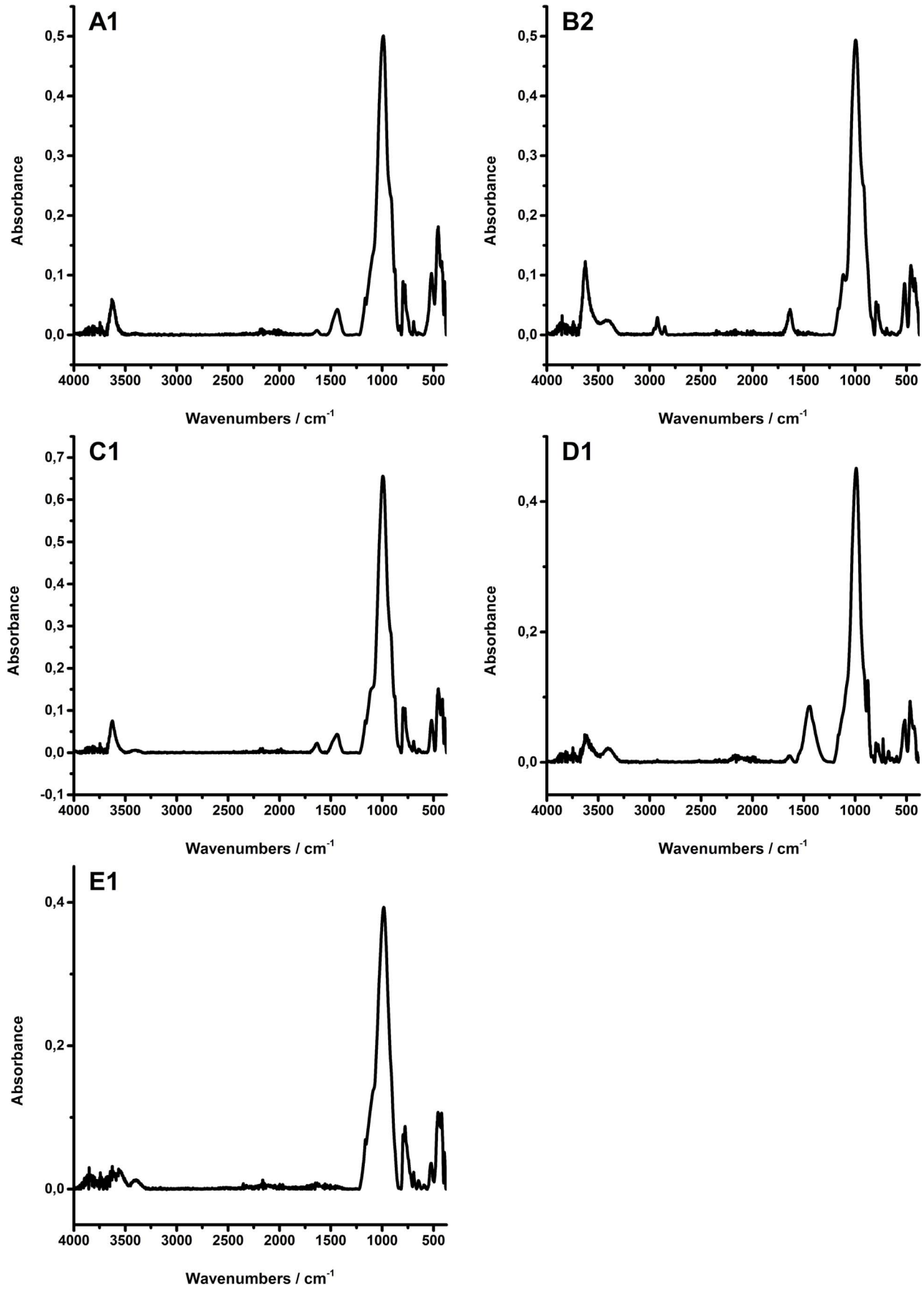

Figure 2 | Infrared spectra of samples from each shale group.

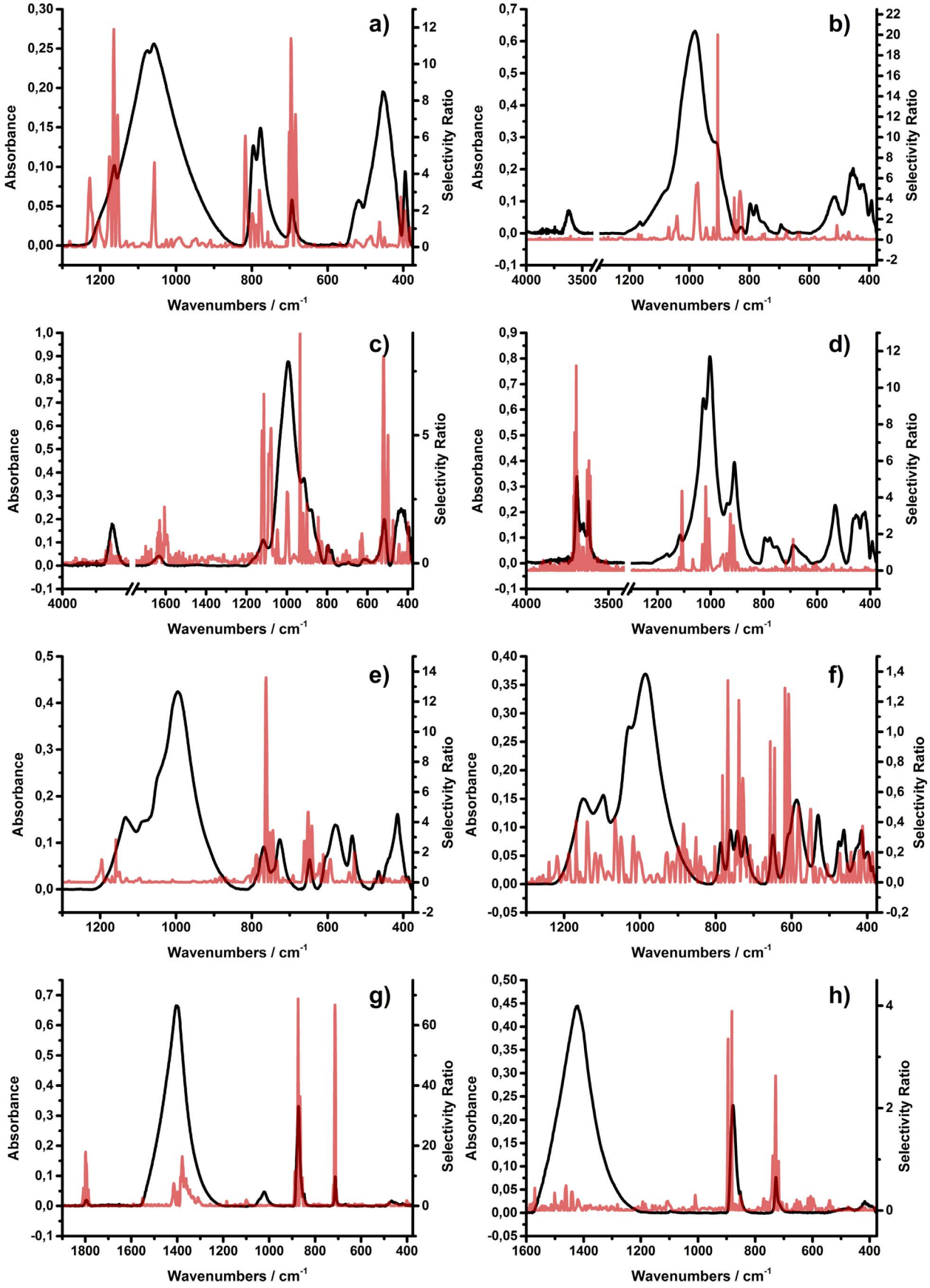

Figure 3 | Mineral spectra of (a) quartz, (b) illite, (c) montmorillonite, (d) kaolinite, (e) albite, (f) orthoclase, (g) calcite and (h) dolomite (black) with respective selectivity ratios (red).

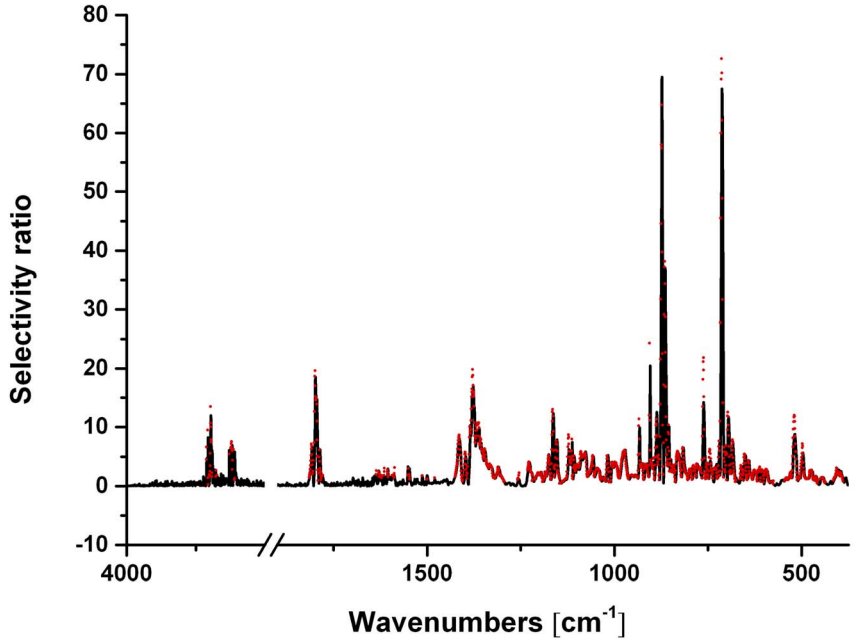

Figure 4 | **Selectivity ratios including the whole spectral range (black) vs. new model with limited wavenumbers (red).**

Besides the mineral phases considered herein (i.e., quartz, illite, smectite, kaolinite, albite, orthoclase, calcite, and dolomite), the shale samples also contained varying amounts of siderite, anatase, pyrite, chlorite, hematite, and anhydrite. With few exceptions, the content of these minerals in the shales was determined to be <5%.

The shales analyzed in this study were obtained from five different locations. Spectra of selected shale samples representing each location are given in **Figure 2**. Clay minerals are readily indentified via the vibration at 3600 cm^{-1}. It is not possible to discriminate illite and smectites in such complex natural mixtures, whereas kaolinite may be easily identified in sample E1. Sample A1, C1, and D1 contain carbonate. Using the weak signals at 713 cm^{-1}, calcite was identified in A1 and D1, as well as dolomite in C1 using the signal at 727 cm^{-1}. Sample B2 apparently contains remains of organic matter, as evidenced by the C–H vibration at 2950 to 2850 cm^{-1}. The vibrational bands arising from the organic matter occur in a different region of the IR spectra, and this should in principle render the determination of the mineral content of the shale samples less problematic. All shales show overlapping absorption features in the spectral range of 1200 to 375 cm^{-1}. Hence, for unambiguous signature assignment of quartz, clays and feldspars multivariate data analysis within this spectral region is required.

Multivariate data analysis. The aim of this study was to provide a straightforward strategy for the evaluation of the mineralogy of shale samples via IR-ATR spectra. However, as the main structural units of these minerals are based on Si–O bonds, most relevant IR absorption features overlap rendering simultaneous quantification somewhat challenging. Therefore, a multivariate regression model based on PLS using the SIMPLS algorithm was established capable of extracting the unique spectral features for each mineral spectrum facilitating identification[41]. Eight latent variables (LVs) were selected, which captured 93.92% of the variance within the calibration data set. Applying a 2nd derivative Savitzky-Golay filter to reduce interferences from noise and mean centring to pre-process the spectra yielded a robust calibration model. The calibration was validated using cross-validation, i.e., random samples of the calibration set were removed from the model, and were then validated via a model built from the remaining calibration data set. In addition, a number of mineral mixtures were prepared to evaluate the predictive capabilities of the model, as discussed later.

Establishing initial calibration models, it was found that the prediction for the validation set were acceptable, deviating by 1–5% from the initial weight, whereas the calibration yielded less satisfying results for the shale samples with errors up to 20%. This is associated with using the entire IR spectra (4000–375 cm^{-1}) for establishing the calibration model calibration. The real-world shale spectra include information that is not captured by the calibration model, which predominantly results from organic matter and absorption features caused by minerals not considered within the model. One option for minimizing the influence of non-calibrated signals is to reduce the spectral range (i.e., spectral region selection), and thereby eliminate wavelengths that do not contribute relevant information[42]. Yet, it was necessary to investigate which regions of the spectra could be omitted without compromising the predictive capabilities of the calibration model.

The usefulness of variables within a calibration model may be rated using so-called selectivity ratios, i.e., a numerical assessment of the relevance of each variable[43]. The larger the value of the selectivity ratio, the more relevant the associated wavelength is considered for prediction. Wavelengths with low selectivity ratios may therefore be left out to improve the model performance. Consequently, the selectivity ratios for each mineral were calculated and compared to the corresponding IR spectra, which are shown in **Figure 3**. The selectivity ratios correlate well with the corresponding spectra, thus enabling the identification of the relevant wavelengths to be used by the model for predicting each mineral species. For minerals with a unique absorption feature like the sharp –OH interlayer vibrations of the kaolinite species or the CO_3^{2-} vibrations of the carbonate minerals, one would readily expect that the model focuses on such pronounced spectral features for calibration. However, for the other minerals with less distinct signatures these plots reveal excellent insight on the wavelengths that are most relevant for each specific mineral. It is crucial to note that the overall selectivity ratios for orthoclase and dolomite are very low – max. 1.3 and 3.8, respectively, which leads to the assumption that the predictive power for those minerals will be moderate within the final calibration model even after spectral region selection.

Table 1 | Calibration statistics for each mineral component

[wt%]	RMSEC	RMSECV	R^2	RMSEP - Validation	RMSEP - Shale
Quartz	2.2	2.7	0.979	4.0	5.7
Illite	2.0	2.3	0.986	2.5	17.2
Montmorillonite	2.3	3.0	0.982	3.6	14.6
Kaolinite	1.2	1.4	0.962	1.7	2.3
Albite	0.9	1.1	0.984	1.2	3.1
Orthoclase	1.9	2.2	0.857	1.9	4.0
Calcite	1.0	1.3	0.994	1.8	2.4
Dolomite	1.6	1.9	0.927	4.3	4.0

Finally, the selectivity ratios for each mineral were added up, and a threshold of 1 was selected as a limit for the wavelengths to be included into further modelling (**Figure 4**). A significant spectral region was excluded from establishing the final calibration model (i.e., the spectral range from 3500 to 1700 cm^{-1} along with several wavenumbers within the remaining regions).

Using this strategy of spectral region selection, a new calibration model was established, as summarized in **Table 1**. The root mean square error of calibration (RMSEC) indicates how well the established model fits the data set, whereas the root mean square error of cross validation (RMSECV) indicates how well the model predicts samples that were not included during the model development. As expected from the low selectivity ratios, the regression quality of orthoclase and dolomite are moderate with a coefficient of determination of 0.857 and 0.927, respectively.

In their work on a chemometric analysis of mineral constituents on simulated oil shales, Palayangoda and Ngyuen used a PCR model to quantify the main components and obtained RMSEC and R^2 values ranging from 0.574–1.501 wt% and 0.977–0.991 respectively[24]. However, their analysis included only five components and the minerals used for calibration modelling were not revised on impurities.

Given that the mineral standards from which the regression model was calculated were of natural origin and contained impurities along with overlapping spectral features, the coefficients of determination (R^2) ranging from 0.857 to 0.994 are highly satisfying.

However, even after spectral region selection the shale spectra still contain residuals that are not fully explained by the calibration model, as can be inferred from **Figure 5**. The Q residuals indicate the residual between the sample and its projection into the latent variable space. The Q residuals of all shale samples are outside the 95% confidence limit. Consequently and importantly, it is shown herein that a model established based on almost pure mineral samples may only describe details of a complex real-world matrix such as shales to a certain extent. The root mean square error of prediction (RMSEP) for the validation and the shale set are summarized in **Table 1**.

The calculated regression functions along with the validation data set and the shale data are shown in **Figure 6**.

The wt% for the prediction of the IR-ATR measurements compared to the initial weight is given in **Table 2**. Evidently, the initial weight does not sum up to 100 wt% for all validation samples, as only the eight minerals of interest were considered. In turn, few predictions resulted in negative wt% values (e.g., a dolomite content of −7% was predicted for sample Val.-6). Negative predictions were predominant for dolomite resulting from the limitations of the calibration model even after spectral region selection, were therefore set to 0 wt%. For the remaining samples within the validation data set the established calibration model yields satisfying results that are in agreement with the specified weight. The finally obtained results of the IR-ATR studies are summarized in **Table 2**.

Discussion

Noteworthy is the prediction error for illite and smectites within the natural shale samples. While the illite content throughout all shale samples is over predicted, the results for smectite with the exception

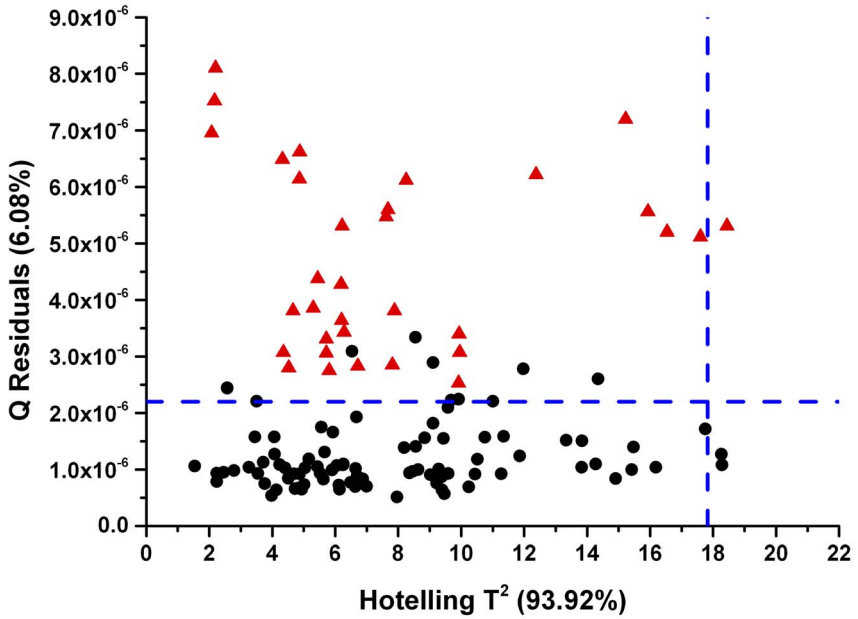

Figure 5 | Hotelling T^2 vs Q Residuals plot. Calibration set (black dots), shale set (red triangles) and confidence limit (blue dashed line).

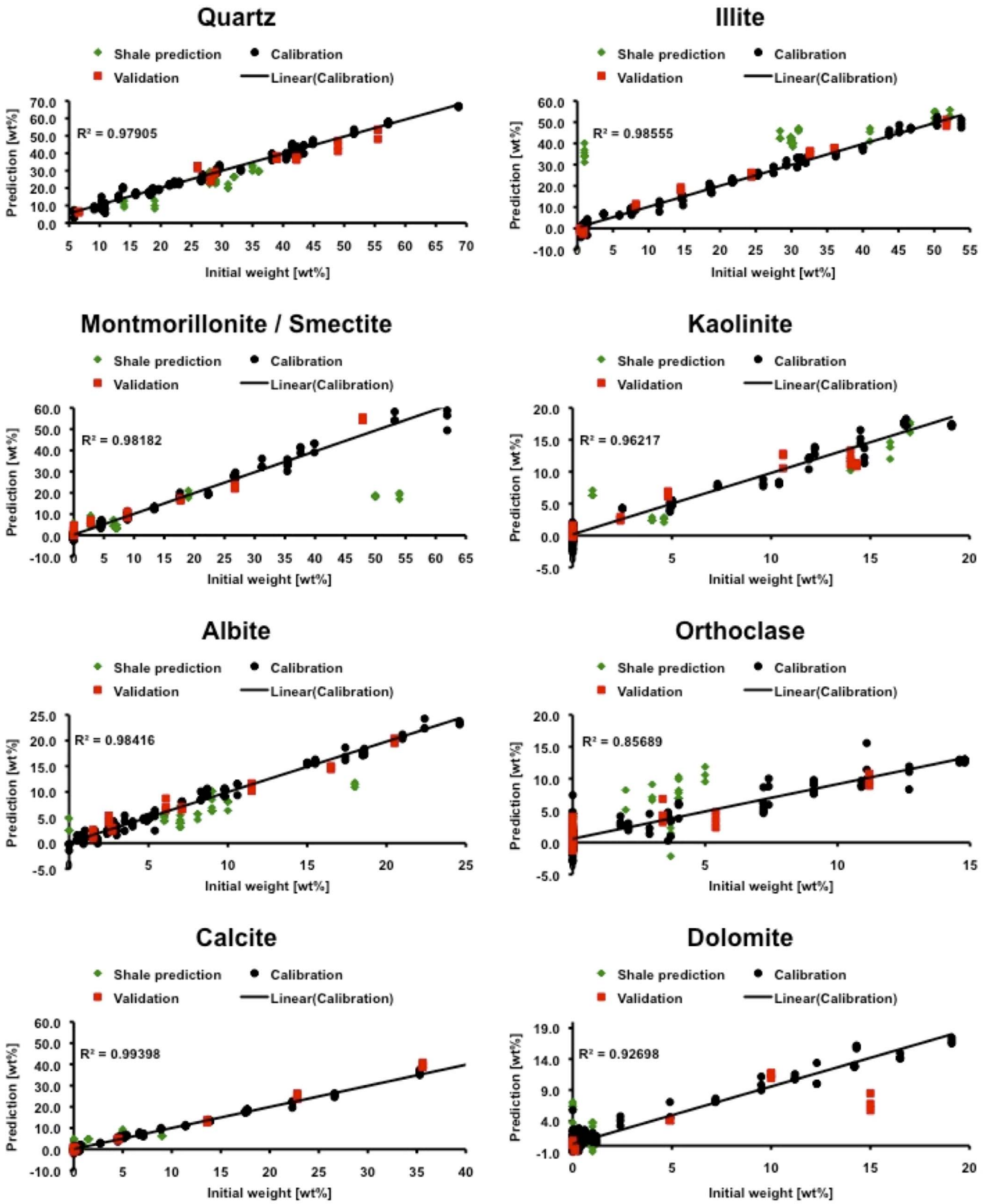

Figure 6 | **Regression lines calculated by the PLS model.**

of group A and D are under predicted, although the prediction error of illite and montmorillonite content in the validation set was at 2.5 and 3.6 wt%, respectively. Similar issues were experienced by Kaufhold et al. (2012)[13]. Based on 57 reference materials, manual pattern addition of the respective IR spectra was used to quantify the mineralogical composition of real world bentonites and clays. Due to the similarity of the illite and smectite IR spectra, the sum of both minerals was determined instead of the individual content.

Table 2 | Comparison between the initial weight [I.W.] or XRD results and the results of the infrared [IR] prediction, respectively. The results of the IR prediction are given as mean ± standard deviation

Sample	[wt%]	Quartz	Illite	Montmorillonite/ Smectite	Kaolinite	Albite	Orthoclase	Calcite	Dolomite
Val.-1	IR	51.8 ± 2.6	25.4 ± 0.8	2.4 ± 0.3	12.2 ± 0.9	7.4 ± 0.9	2.3 ± 1.1	0.7 ± 0.2	0.0 ± 0.6
	I.W.	55.5	24.4	0.0	14.0	6.1	0.0	0.0	0.0
Val.-2	IR	25.0 ± 1.3	0 ± 0.8	54.7 ± 0.6	12.0 ± 1.0	10.9 ± 0.6	0.3 ± 1.0	0.0 ± 0.2	0.0 ± 1.8
	I.W.	28.2	0.8	47.9	10.6	11.5	0.0	0.0	0.0
Val.-3	IR	44.2 ± 2.5	37.6 ± 0.2	6.4 ± 0.5	1.0 ± 0.6	6.7 ± 0.2	0.4 ± 0.5	4.8 ± 0.3	0.0 ± 1.7
	I.W.	49.0	36.0	2.8	0.0	7.1	0.0	4.5	0.1
Val.-4	IR	36.9 ± 0.5	49.7 ± 1.3	4.3 ± 0.4	0.2 ± 0.4	2.8 ± 0.2	4.8 ± 1.5	0.7 ± 0.2	0.4 ± 0.3
	I.W.	42.2	51.7	0.0	0.0	2.7	3.4	0.0	0.0
Val.-5	IR	28.7 ± 0.3	35.7 ± 0.7	10.1 ± 1.2	2.6 ± 0.2	14.7 ± 0.2	3.6 ± 1.0	0.1 ± 0.1	4.1 ± 0.1
	I.W.	28.8	32.6	8.9	2.4	16.5	5.4	0.2	4.9
Val.-6	IR	32.1 ± 0.5	0.0 ± 0.5	22.9 ± 0.7	6.6 ± 0.4	1.8 ± 0.6	0.1 ± 1.0	39.8 ± 0.8	0.0 ± 0.9
	I.W.	26.0	0.4	26.7	4.8	1.5	0.0	35.6	0.8
Val.-7	IR	37.7 ± 0.7	10.5 ± 0.7	0.3 ± 0.1	9.3 ± 0.2	4.6 ± 0.6	9.9 ± 0.8	13.2 ± 0.4	11.4 ± 0.4
	I.W.	39.0	8.2	0.0	14.3	2.5	11.2	13.6	10.0
Val.-8	IR	6.3 ± 0.3	18.5 ± 0.6	16.8 ± 0.4	0.1 ± 0.2	20.0 ± 0.4	3.0 ± 0.9	25.2 ± 1.1	7.0 ± 1.1
	I.W.	6.6	14.5	17.7	0.0	20.5	0.0	22.8	15.0
A-1	IR	29.1 ± 0.4	50.3 ± 1.0	7.1 ± 0.9	0.3 ± 0.4	4.6 ± 0.6	3.0 ± 1.0	6.6 ± 0.2	0.0 ± 0.0
	XRD	28.0	50.1	2.9	0.0	7.0	0.0	5.0	1.0
A-2	IR	25.3 ± 0.8	54.0 ± 1.3	5.2 ± 0.5	0.4 ± 0.4	3.4 ± 0.4	3.0 ± 1.2	8.8 ± 0.4	0.1 ± 0.2
	XRD	28.0	50.1	2.9	0.0	7.0	0.0	5.0	1.0
A-3	IR	24.8 ± 0.3	53.7 ± 1.5	6.3 ± 2.2	0.0 ± 0.0	4.6 ± 0.3	3.0 ± 1.7	6.3 ± 0.2	0.8 ± 0.7
	XRD	27.0	52.2	2.8	0.0	6.0	0.0	9.0	1.0
B-1	IR	10.3 ± 2.0	37.5 ± 1.9	18.7 ± 1.2	6.6 ± 0.4	9.6 ± 0.8	9.5 ± 0.9	0.7 ± 0.4	6.6 ± 0.3
	XRD	19.0	1.0	54.0	1.0	9.0	4.0	0.0	0.0
B-2	IR	26.5 ± 0.3	33.0 ± 1.3	18.4 ± 0.4	2.5 ± 0.2	5.2 ± 1.4	7.2 ± 0.4	0.5 ± 0.3	6.2 ± 0.4
	XRD	32.0	1.0	50.0	4.0	7.0	4.0	0.0	0.0
C-1	IR	23.4 ± 0.9	41.8 ± 0.7	19.1 ± 1.4	2.5 ± 0.3	5.3 ± 0.5	0.5 ± 0.7	4.8 ± 0.2	1.6 ± 1.2
	XRD	29.0	30.0	19.0	4.6	8.1	3.7	1.5	1.0
D-1	IR	10.7 ± 1.5	44.5 ± 2.6	5.2 ± 0.5	0.4 ± 0.3	3.2 ± 1.1	10.7 ± 1.0	4.4 ± 0.5	20.6 ± 0.8
	XRD	14.0	41.0	0.0	0.0	0.0	5.0	0.0	29.0
E-1	IR	31.6 ± 1.4	39.5 ± 0.8	5.9 ± 0.5	0.6 ± 0.6	11.4 ± 0.4	7.6 ± 1.1	1.3 ± 0.3	1.9 ± 1.3
	XRD	35.0	30.2	4.8	0.0	18.0	3.0	0.0	0.0
E-2	IR	29.8 ± 0.4	42.0 ± 1.2	3.7 ± 0.8	11.3 ± 0.8	5.4 ± 0.1	5.3 ± 2.4	1.7 ± 0.2	0.6 ± 0.7
	XRD	36.0	29.9	7.1	14.0	6.0	2.0	1.0	0.0
E-3	IR	23.4 ± 1.3	46.5 ± 0.6	3.9 ± 0.8	17.1 ± 0.7	6.5 ± 0.3	0.7 ± 0.5	1.3 ± 0.4	0.6 ± 0.5
	XRD	28.0	31.0	7.0	17.0	9.0	0.0	0.0	1.0
E-4	IR	20.7 ± 1.1	43.6 ± 1.6	5.5 ± 1.4	13.5 ± 1.1	7.5 ± 0.8	4.3 ± 0.2	1.5 ± 0.6	3.1 ± 0.9
	XRD	31.0	28.4	6.6	16.0	10.0	0.0	0.0	1.0

Their established method overestimated the content of the illite+smectite and it was presumed that using illite/smectite mixed layer minerals for calibration, instead of the pure smectite or illite, should yield better results. A possible influence of mixed layer illite+smectite could not be investigated, as no illite/smectite mixed layer minerals were available for calibration in the present study. As the most abundant representative of the smectite minerals, montmorillonite was used for calibration purposes[44]. However, montmorillonite is not necessarily the only smectite occurring within the studied shale samples, and since spectral differences between different smectites are existing (e.g., Fe-related vibrations in nontronite[45]) an influence of different smectite minerals cannot be excluded. However, it is anticipated that larger calibration data sets combining neat mineral samples (without impurities) and synthetic mixtures more closely resembling the variance of natural shale samples along with improved chemometric algorithms will assist minimizing these effects in future. Nonetheless, satisfactory results were achieved for most of the minerals, thus demonstrating the potential and utility of the developed methodology for the direct analysis of shales via IR-ATR spectroscopy and multivariate data analysis.

Using IR-ATR spectra, a multivariate calibration model for direct mineral composition identification was developed from 30 pure mineral mixtures facilitating the simultaneous quantification of 8 different minerals. After validation, the model was then applied to predict the composition of 11 natural shale samples providing data in excellent agreement with associated XRD studies. Recent achievements by Washburn et al.[27] combining ATR-FTIR and multivariate analysis, show that the combination of IR-ATR spectroscopy as a direct analytical technique requiring only little sample preparation combined with multivariate data analysis offers a rapid and less destructive methodology for the analysis OF ORGANIC CONSTITUENTS of shale rocks. As the general rock composition and properties play a crucial role in determining the economic viability of shales in terms of their content in gas and/or oil that may be harvested from such composites, the presented methodology provides an interesting strategy for the rapid assessment of mineral constituents.

Methods

Materials and reagents. A series of natural reference minerals were used in this study for calibration purposes, and for mineral quantification in shales. However, even the reference minerals were contaminated with impurities (i.e., other minerals), which had to be considered when developing the calibration model. The following minerals with provided purity in brackets were studied: calcite (89%), kaolinite (96%), dolomite (95%), quartz (99%), orthoclase (73%), montmorillonite (89%), albite (98%) and illite (<72%). Since montmorillonite was used to establish the calibration model, the term montmorillonite is used whenever an unambiguous assignment of the mineral is possible; smectite is used, if the assignment is not unambiguous. All reference materials were obtained from Sibelco Australia, Ward's Natural Science (Illinois) and Worker Ceramics Australia and used as purchased. A total of 11 natural

shale rock samples collected at 5 different locations were also analyzed and labelled as sample A to E, respectively.

Instrumentation. IR-ATR measurements were collected using a Bruker Alpha FTIR spectrometer (Bruker Optics GmbH, Ettlingen, Germany) equipped with a deuterated triglycine sulfate (DTGS) detector. The Alpha-P ATR accessory is equipped with a single-reflection diamond ATR hemisphere and a spring-loaded mechanical press for compacting solid samples at the ATR waveguide surface with uniform and reproducible pressure. Data were recorded in the MIR spectral range from 4000–375 cm^{-1} at a spectral resolution of 2 cm^{-1}. 200 scans were averaged for background and sample spectra, respectively. All experiments were performed at ambient conditions (T = 21 ± 1°C).

XRD measurements were collected using a PANalytical X'Pert Pro multipurpose X-ray diffractometer using Fe filtered Co Ka radiation, 1/4° divergence slit, 1/2° antiscatter slit and X'Celerator Si strip detector. Details of the acquisition procedure are given in Delle Piane et al.[46] Quantitative analysis was performed on the XRD data using the commercial software package SIROQUANT from Sietronics Pty Ltd.

Sample preparation. For establishing calibration and validation samples, the obtained reference minerals were mixed at different compositions, homogenized for 10 min using an agate mortar and pestle, as too extensive grinding can cause amorphization or particle size related shifts in the IR spectra[13,47]. In total, 30 different mixtures were prepared for establishing the calibration model. The calibration samples were prepared to match the mineral content usually found within natural shale samples. The compositional range of the minerals used for preparing the calibration samples was as follows: quartz (10–55 wt%), illite (0–55 wt%), montmorillonite (0–60 wt%), kaolinite (0–15 wt%), albite (0–25 wt%), orthoclase (0–15 wt%), calcite (0–55 wt%) and dolomite (0–20 wt%).

In addition, eight mixtures were prepared as model validation samples, and 11 natural shale samples were prepared as real-world examples analysed at the same conditions. Prior to any solid sample deposition, the surface of the diamond ATR waveguide was cleaned by soaking with acetone and wiped using lens-cleaning tissues (Whatman International Ltd., Maidstone, England). Prior to recording background spectra, acetone was allowed to evaporate for at least 15 min. For each measurement, approx. 100 mg of solid dry sample was firmly pressed against the waveguide surface. Each sample spectrum was independently recorded three times to ensure reproducibility of the measurement procedure.

For XRD measurements of the shale rocks, bulk samples were pre-ground for 15 seconds in a tungsten carbide mechanical mill, and passed through a 0.5 mm sieve. A 1 g sub-sample was further ground for 10 minutes in a McCrone micronizing mill under ethanol. The resulting slurry was oven dried at 60°C, and then thoroughly mixed in an agate mortar and pestle before being lightly pressed into stainless steel sample holders for X-ray diffraction analysis (see details in Delle Piane et al.[46]).

Multivariate calibration and data analysis. The obtained IR spectral data was pre-processed using the software package OPUS (Bruker Optics GmbH, Ettlingen, Germany). Atmospheric compensation for reducing the influence of CO_2 and H_2O absorption bands, and baseline correction was applied to every recorded spectrum prior to multivariate analysis. The multivariate analysis was performed using the PLS toolbox (Eigenvector Research, Wenatchee, WA, USA) for MatLab (MathWorks Inc., Natick, MA, USA) using the entire spectral range from 4000–375 cm^{-1}. A linear regression model was established using partial least squares (PLS) with the SIMPLS algorithm based on 8 latent variables using 90 calibration spectra. Prior to evaluating natural shales based on this model, the quality of the model was tested using the validation sample set.

1. Warwick, P. D. Unconventional Energy Resources: 2011 Review. *Nat. Resour. Res.* **20**, 279–328 (2011).
2. Leather, D. T. B., Bahadori, A., Nwaoha, C. & Wood, D. A. A review of Australia's natural gas resources and their exploitation. *J. Nat. Gas Sci. Eng.* **10**, 68–88 (2013).
3. Tissot, B. P. *Petroleum Formation and Occurrence A New Approach to Oil and Gas Exploration.* (Springer Berlin Heidelberg, 1978).
4. Bustin, A. M. M. & Bustin, R. M. Importance of rock properties on the producibility of gas shales. *Int. J. Coal Geol.* **103**, 132–147 (2012).
5. Yaalon, D. H. Mineral composition of the average shale. *Clay Miner. Bull.* **5**, 31–36 (1962).
6. Josh, M., Esteban, L., Delle Piane, C., Sarout, J., Dewhurst, D. N. & Clennell, M. B. Laboratory characterisation of shale properties. *J. Pet. Sci. Eng.* **88–89**, 107–124 (2012).
7. Bhargava, S., Awaja, F. & Subasinghe, N. Characterisation of some Australian oil shale using thermal, X-ray and IR techniques. *Fuel* **84**, 707–715 (2005).
8. Wang, D.-M., Xu, Y.-M., He, D.-M., Guan, J. & Zhang, O.-M. Investigation of mineral composition of oil shale. *Asia-Pac. J. Chem. Eng.* **4**, 691–697 (2009).
9. Mandile, A. J. & Hutton, A. C. Quantitative X-ray diffraction analysis of mineral and organic phases in organic-rich rocks. *Int. J. Coal Geol.* **28**, 51–69 (1995).
10. Patterson, J. H. & Henstridge, D. A. Comparison of the mineralogy and geochemistry of the Kerosene Creek Member, Rundle and Stuart oil shale deposits, Queensland, Australia. *Chem. Geol.* **82**, 319–339 (1990).
11. Dewhurst, D. N., Jones, R. M. & Raven, M. D. Microstructural and petrophysical characterization of Muderong Shale: application to top seal risking. *Pet. Geosci.* **8**, 371–383 (2002).
12. Kahle, M., Kleber, M. & Jahn, R. Review of XRD-based quantitative analyses of clay minerals in soils: the suitability of mineral intensity factors. *Geoderma* **109**, 191–205 (2002).
13. Kaufhold, S., Hein, M., Dohrmann, R. & Ufer, K. Quantification of the mineralogical composition of clays using FTIR spectroscopy. *Vib. Spectrosc.* **59**, 29–39 (2012).
14. Thornley, D. M. & Primmer, T. J. Thermogravimetry/evolved water analysis (TG/EWA) combined with XRD for improved quantitative whole-rock analysis of clay minerals in sandstones. *Clay Miner.* **30**, 27–38 (1995).
15. Frost, R. L., Bahfenne, S. & Graham, J. Infrared and infrared emission spectroscopic study of selected magnesium carbonate minerals containing ferric iron–Implications for the geosequestration of greenhouse gases. *Spectrochim. Acta. A. Mol. Biomol. Spectrosc.* **71**, 1610–1616 (2008).
16. Yitagesu, F. A., van der Meer, F., van der Werff, H. & Hecker, C. Spectral characteristics of clay minerals in the 2.5–14 μm wavelength region. *Appl. Clay Sci.* **53**, 581–591 (2011).
17. Madejova, J. FTIR techniques in clay mineral studies. *Vib. Spectrosc.* **31**, 1–10 (2003).
18. Alstadt, K. N., Katti, D. R. & Katti, K. S. An in situ FTIR step-scan photoacoustic investigation of kerogen and minerals in oil shale. *Spectrochim. Acta. A. Mol. Biomol. Spectrosc.* **89**, 105–113 (2012).
19. Solomon, P. R. & Miknis, F. P. Use of Fourier Transform infrared spectroscopy for determining oil shale properties. *Fuel* **59**, 893–896 (1980).
20. Shoval, S. & Nathan, Y. Analyzing the calcination of sulfur-rich calcareous oil shales using FT-IR spectroscopy and applying curve-fitting technique. *J. Therm. Anal. Calorim.* **105**, 883–896 (2011).
21. Brown, J. M. & Elliott, J. J. Quantitative analysis of minerals in oil shales by fourier transform infrared spectroscopy. in *Prepr Pap Am Chem Soc Div Pet Chem* **32**, 65–70 (1987).
22. Snyder, R. W., Painter, P. C. & Cronauer, D. C. Development of FT-ir procedures for the characterization of oil shale. *Fuel* **62**, 1205–1214 (1983).
23. Bertaux, J., Frohlich, F. & Ildefonse, P. Multicomponent analysis of FTIR spectra: quantification of amorphous and crystallized mineral phases in synthetic and natural sediments. *J. Sediment. Res.* **68** (1998).
24. Palayangoda, S. S. & Nguyen, Q. P. An ATR-FTIR Procedure for Quantitative Analysis of Mineral Constituents and Kerogen in Oil Shale. *Oil Shale* **29**, 344 (2012).
25. Klinkenberg, M., Dohrmann, R., Kaufhold, S. & Stanjek, H. A new method for identifying Wyoming bentonite by ATR-FTIR. *Appl. Clay Sci.* **33**, 195–206 (2006).
26. Adams, M. J., Awaja, F., Bhargava, S., Grocott, S. & Romeo, M. Prediction of oil yield from oil shale minerals using diffuse reflectance infrared Fourier transform spectroscopy. *Fuel* **84**, 1986–1991 (2005).
27. Washburn, K. E. & Birdwell, J. E. Multivariate analysis of ATR-FTIR spectra for assessment of oil shale organic geochemical properties. *Org. Geochem.* **63**, 1–7 (2013).
28. Ganz, H. H. & Kalkreuth, W. IR classification of kerogen type, thermal maturation, hydrocarbon potential and lithological characteristics. *J. Southeast Asian Earth Sci.* **5**, 19–28 (1991).
29. Khan, M. R., Seshadri, K. S. & Kowalski, T. E. Comparative study on the compositional characteristics of pyrolysis liquids derived from coal, oil shale, tar sand, and heavy residue. *Energy Fuels* **3**, 412–420 (1989).
30. Saikia, B. J., Parthasarathy, G. & Sarmah, N. C. Fourier transform infrared spectroscopic estimation of crystallinity in SiO2 based rocks. *Bull. Mater. Sci.* **31**, 775–779 (2008).
31. Srasra, E., Bergaya, F. & Fripiat, J. J. Infrared spectroscopy study of tetrahedral and octahedral substitutions in an interstratified illite-smectite clay. *Clays Clay Miner.* **42**, 237–241 (1994).
32. Cuadros, J. & Altaner, S. P. Compositional and structural features of the octahedral sheet in mixed-layer illite/smectite from bentonites. *Eur. J. Mineral.* **10**, 111–124 (1998).
33. Pironon, J., Pelletier, M., de Donato, P. & Mosser-Ruck, R. Characterization of smectite and illite by FTIR spectroscopy of interlayer NH4+ cations. *Clay Miner.* **38**, 201–211 (2003).
34. Vaculikova, L., Plevova, E., Vallova, S. & Koutnik, I. Characterization and differentiation of kaolinites from selected Czech deposits using infrared spectroscopy and differential thermal analysis. *Acta Geodyn. Geomater.* **8**, 59–67 (2011).
35. Balan, E. First-principles study of OH-stretching modes in kaolinite, dickite, and nacrite. *Am. Mineral.* **90**, 50–60 (2005).
36. McKeown, D. A. Raman spectroscopy and vibrational analyses of albite: From 25 C through the melting temperature. *Am. Mineral.* **90**, 1506–1517 (2005).
37. Matteson, A. & Herron, M. M. End-Member Feldspar Concentrations Determined by FTIR Spectral Analysis. *J. Sediment. Petrol.* **63**, 1144–1148 (1993).
38. Chester, R. & Elderfield, H. The Application of Infra-Red Absorption Spectroscopy To Carbonate Mineralogy. *Sedimentology* **9**, 5–21 (1967).
39. Luzinova, Y., Dobbs, G. T., Lapham, L., Chanton, J. P. & Mizaikoff, B. Detection of cold seep derived authigenic carbonates with infrared spectroscopy. *Mar. Chem.* **125**, 8–18 (2011).
40. Farmer, V. C. The Infra-red Spectra of Talc, Saponite, and Hectorite. *Mineral. Mag.* **31**, 829–845 (1958).
41. De Jong, S. SIMPLS: An alternative approach to partial least squares regression. *Chemom. Intell. Lab. Syst.* **18**, 251–263 (1993).

42. Seichter, F. *et al.* Multivariate determination of 13CO2/12CO2 ratios in exhaled mouse breath with mid-infrared hollow waveguide gas sensors. *Anal. Bioanal. Chem.* **405**, 4945–4951 (2013).
43. Rajalahti, T. *et al.* Biomarker discovery in mass spectral profiles by means of selectivity ratio plot. *Chemom. Intell. Lab. Syst.* **95**, 35–48 (2009).
44. Weaver, C. E. *Clays, Muds, and Shales.* (Elsevier: Distributors for the U.S. and Canada, Elsevier Science Pub. Co., 1989).
45. Stubican, V. & Roy, R. Infrared Spectra of Layer-Structure Silicates. *J. Am. Ceram. Soc.* **44**, 625–627 (1961).
46. Piane, C. D., Dewhurst, D. N., Siggins, A. F. & Raven, M. D. Stress-induced anisotropy in brine saturated shale: Anisotropy in shales. *Geophys. J. Int.* **184**, 897–906 (2011).
47. Müller, C. M. *et al.* Infrared Attenuated Total Reflection Spectroscopy of Quartz and Silica Micro- and Nanoparticulate Films. *J. Phys. Chem. C* **116**, 37–43 (2012).

Acknowledgments

The authors greatly acknowledge funding provided by the Capability Development Fund at CESRE, and the CSIRO Wealth from Oceans Flagship. BM particularly acknowledges an OCE Distinguished Visiting Scientist Fellowship for an extended research stay at CSIRO, Perth, Australia.

Author contributions

B.P. and B.M. developed the project. C.M.M., B.P. and B.M. have planned, performed and discussed the IR experiments, L.E., C.D.P. and M.R. the XRD experiments, respectively. C.M.M., B.P. and B.M. have written the manuscript. All authors contributed to manuscript revision.

Additional information

Competing financial interests: The authors declare no competing financial interests.

How to cite this article: Müller, C.M. *et al.* Infrared Attenuated Total Reflectance Spectroscopy: An Innovative Strategy for Analyzing Mineral Components in Energy Relevant Systems. *Sci. Rep.* **4**, 6764; DOI:10.1038/srep06764 (2014).